

ALPHA AND CLUSTER DECAY HALF LIVES IN TUNGSTEN ISOTOPES: A MICROSCOPIC ANALYSIS

NITHU ASHOK*, ANTONY JOSEPH

*Department of Physics, University of Calicut,
Kerala, India*

Abstract

Alpha and cluster decay half-lives for Tungsten (W) isotopes in the range between 2p drip line and beta stability line are studied. The sensitivity of different Skyrme parametrizations in predicting the alpha-decay and probable cluster decay modes from W isotopes have been analysed. The half-lives are calculated using UDL. Predicted half-lives are compared with ELDM and also with available experimental values. The use of HO and THO basis do not produce much differences in the results. The study also revealed the role of neutron shell closure in cluster decay process.

Keywords: cluster; Q-value; half-life, Hartree-Fock-Bogoliubov.

1. Introduction

Cluster radioactivity is defined as the spontaneous emission of a fragment, heavier than alpha particle and lighter than the lightest fission fragment, from the parent nuclei, without being accompanied by neutron emission. This phenomenon was first predicted by Sandulescu et.al in 1980[1]. This exotic decay was later experimentally observed by Rose and Jones[2] in 1984, with the emission of ^{14}C cluster from ^{223}Ra . Cluster radioactivity is a cold nuclear phenomenon, explained based on quantum mechanical fragmentation theory

*Corresponding author
URL: nithu.ashok@gmail.com (NITHU ASHOK)

(QMFT)[3, 4]. One of the dominant decay modes in nuclei is the α -decay, which is the emission of ${}^4_2\text{He}$ from the parent nuclei. The probability of formation of a cluster is mainly determined by its binding energy. This implies that of all the possible cluster emissions, α -cluster is the most prominent one.

Many theoretical models have been developed to study the phenomenon of cluster radioactivity. The widely used phenomenological models are Preformed Cluster Model (PCM)[5] and Unified Fission Model (UFM)[6]. In PCM, the cluster is assumed to be preformed inside the parent nucleus and the preformation probability has to be found out explicitly. In UFM, the parent nucleus undergoes continuous dynamical changes through a molecular phase and finally disintegrates into a daughter and a cluster. Here the preformation probability is taken as unity. Several theoretical and experimental studies on cluster decay have been carried out in recent years. Different studies show that this phenomenon occurs in those regions where daughter nuclei should either be doubly magic or in its vicinity.

In our previous work, we have analysed the different decay modes in Os isotopes using Hartree-Fock-Bogoliubov (HFB) theory[10]. In the present work, the feasibility of alpha and cluster decay from W isotopes have been studied using HFB theory. Many works, both theoretical and experimental, have been devoted to the study of alpha decay from various W nuclei in recent years[7, 8, 9]. Here we made an attempt to study the different cluster decay modes from W isotopes in a systematic way with the help of Skyrme HFB theory.

The paper is organised as follows. In sec. 2, a brief account of the microscopic theory (HFB theory) which is used for the present study is given. In sec. 3 we have shown the details of our calculations. Results and discussion are given in sec. 4, where we have presented the main part of the study. In sec. 5, the conclusion drawn from the present work is given.

2. Hartree-Fock-Bogoliubov Theory

A brief description of the Hartree-Fock-Bogoliubov theory is given below. The many body Hamiltonian expressed in terms of annihilation and creation operators is given by[11],

$$H = \sum_{ij} t_{ij} a_i^\dagger a_j + \frac{1}{4} \sum_{ijkl} V_{ijkl} a_i^\dagger a_j^\dagger a_k a_l \quad (1)$$

A set of quasiparticle state is used as the trial wave function. The bare particles are transformed to quasiparticles by using Bogoliubov transformation[11]:

$$\beta_k^\dagger = \sum_l U_{lk} a_l^\dagger + V_{lk} a_l \quad (2)$$

$$\beta_k = \sum_l V_{lk}^* a_l + U_{lk}^* a_l^\dagger \quad (3)$$

In terms of the density matrix ρ and the pairing tensor κ , on which the wavefunction Φ depends, the Hartree-Fock-Bogoliubov energy can be expressed as

$$E[\rho, \kappa] = \frac{\langle \Phi | H - \lambda N | \Phi \rangle}{\langle \Phi | \Phi \rangle} = Tr[(\varepsilon + \frac{1}{2}\Gamma)\rho] - \frac{1}{2}Tr[\Delta\kappa^*] \quad (4)$$

where Hartree Fock(HF) potential Γ and pairing potential Δ are defined as

$$\Gamma_{kl} = \sum_{i,j} \bar{v}_{kjl} \rho_{ij} \quad (5)$$

$$\Delta_{kl} = \frac{1}{2} \sum_{i,j} \bar{v}_{kjl} \kappa_{ij} \quad (6)$$

The HFB equations are obtained by applying the variational principle to $(H - \lambda N)$. In the matrix form, the HFB equation is given by[12],

$$\begin{pmatrix} h - \lambda & \Delta \\ -\Delta^* & -h^* + \lambda \end{pmatrix} \begin{pmatrix} U_n \\ V_n \end{pmatrix} = E_n \begin{pmatrix} U_n \\ V_n \end{pmatrix} \quad (7)$$

where $h = t + \Gamma$, E_n is the quasiparticle energy and λ is the chemical potential.

3. Details of calculation

Skyrme HFB equations have been solved using cylindrically deformed HO and THO basis[13]. The THO set of basis wave functions consist of transformed

harmonic oscillator functions, which are generated by applying the local scale transformation (LST)[14] to the HO single particle wave functions[15]. Numerical calculations have been carried out using 20 oscillator shells. The cut-off energy is taken as 60 MeV. In the particle-hole channel, we have used the zero-range effective Skyrme interactions[16]. In the present work we have used different Skyrme forces like SIII[17], SkP[18], SLy5[19], SkM*[20], UNEDF0[21] and UNEDF1[22]. These Skyrme forces are selected as they are very efficient in reproducing the ground state properties. Also they differ in various parameters and this helps to analyse the effect caused by different factors. They vary in the value of effective mass, surface energy, with the inclusion of J^2 term, centre of mass correction etc. The details of the parameters can be obtained from their corresponding references.

In the particle-particle (pairing) channel, pairing interaction is included using the density dependent delta interaction[23, 24] of the form[25],

$$V_{\delta}^{n/p}(\vec{r}_1, \vec{r}_2) = V_0^{n/p} [1 - \frac{1}{2} (\frac{\rho(\vec{r}_1 + \vec{r}_2)}{\rho_0})^{\alpha}] \delta(\vec{r}_1 - \vec{r}_2) \quad (8)$$

where the saturation density[26] $\rho_0=0.16 \text{ fm}^{-3}$ and $\alpha=1$.

The half-lives corresponding to each decay mode is calculated using a standard formula, the Universal decay law(UDL)[27] which has been deduced from WKB approximations, with some modifications. It is given by,

$$\log_{10} T_{1/2} = a Z_c Z_d \sqrt{\frac{A}{Q}} + b \sqrt{A Z_c Z_d (A_c^{1/3} + A_d^{1/3})} + c \quad (9)$$

where the constants are $a=0.4314$, $b=-0.4087$ and $c=-25.7725$.

Z_c , Z_d are the atomic number of cluster and daughter nuclei, A_c , A_d are the mass number of cluster and daughter nuclei and

$$A = \frac{A_c A_d}{A_c + A_d} \quad (10)$$

Here Q is the Q -value of the decay. Moreover, calculations have been limited to those decays which are having half-lives in the experimentally measurable range ie. $T_{1/2} < 10^{30} \text{ s}$.

4. Results and discussion

In the present study, we have made an attempt to study the feasibility of alpha and cluster decays from Tungsten (W) isotopes. We have analysed all the possible parent-cluster combinations in tungsten isotopes. From a detailed survey carried throughout the isotopic chain, it was found that only those nuclei belonging to the region between proton drip line and beta stability line exhibit these decay modes.

4.1. Alpha decay

At first, we have analysed the feasibility of alpha decay in this isotopic chain because of the availability of the wide range of experimental data. It is found that W isotopes within the mass range 158 to 180 are unstable against alpha decay. Any decay mode will be energetically favourable, if and only if the Q-value is positive. Q_α -values are calculated from binding energies using the relation,

$$Q_\alpha(N, Z) = B(N - 2, Z - 2) + B(2, 2) - B(N, Z) \quad (11)$$

where, $B(N, Z)$ and $B(N-2, Z-2)$ are the binding energies of the parent and the daughter nucleus (${}_{72}\text{Hf}$). $B(2, 2)$, the binding energy of ${}^4_2\text{He}$ nucleus (28.296 MeV) is taken from AME 2012 [28].

The Q-values obtained in the case of different Skyrme forces are given in Table 1. They have been compared with phenomenological Effective Liquid Drop Model (ELDM) [29, 30] values as well as with the available experimental values[31, 32]. A small discrepancy is observed in the estimated Q-values. This is due to the fact that each Skyrme force describes binding energy of W isotopes with slight variation. A small variation in the values of the parameters of the Skyrme forces will affect the values of binding energy. From Table 1, we can see that the values obtained by the recent parametrization, UNEDF0 and UNEDF1 as well as the classical Skyrme parametrization SIII agree with ELDM values. Alpha decay half-lives are calculated using UDL. Logarithmic value of half-lives against mass number of the parent(A) is depicted in Fig. 1. From this

figure, we can observe that the half-life is minimum for ^{158}W , which leads to the magic daughter nuclei ^{154}Hf ($N=82$). It is also visible that except SKM*, all other Skyrme forces overestimate the alpha decay half-lives. We have also studied the standard deviation of the half-lives with respect to experimental values for analysing how much the theoretical values agree with experimental ones. Standard deviations are tabulated in Table 2. From Table 2, it is observed that, SKM* is showing much variation with respect to experimental half-lives, compared to other Skyrme forces.

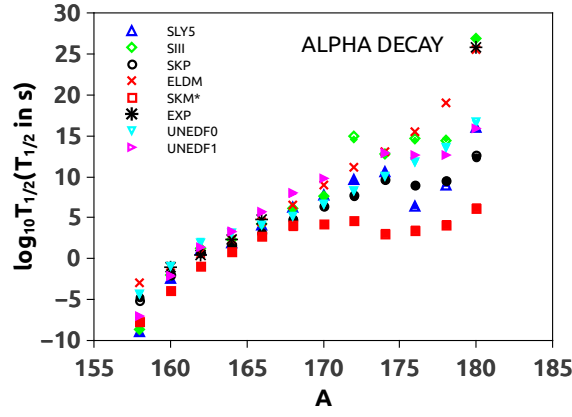


Figure 1: Plots showing logarithmic value of half-life ($T_{1/2}$ in sec) against mass number of parent (A) nuclei corresponding to different decay modes for HO(solid) and THO(open) basis.

4.2. Cluster decay

In W isotopes, we investigated the feasibility of the emission of different clusters like ^8Be , ^{12}C , ^{16}O and ^{20}Ne . The respective Q-values are estimated from binding energy using the following expressions,

^8Be :

$$Q(N, Z) = B(N - 4, Z - 4) + B(4, 4) - B(N, Z) \quad (12)$$

^{12}C :

$$Q(N, Z) = B(N - 6, Z - 6) + B(6, 6) - B(N, Z) \quad (13)$$

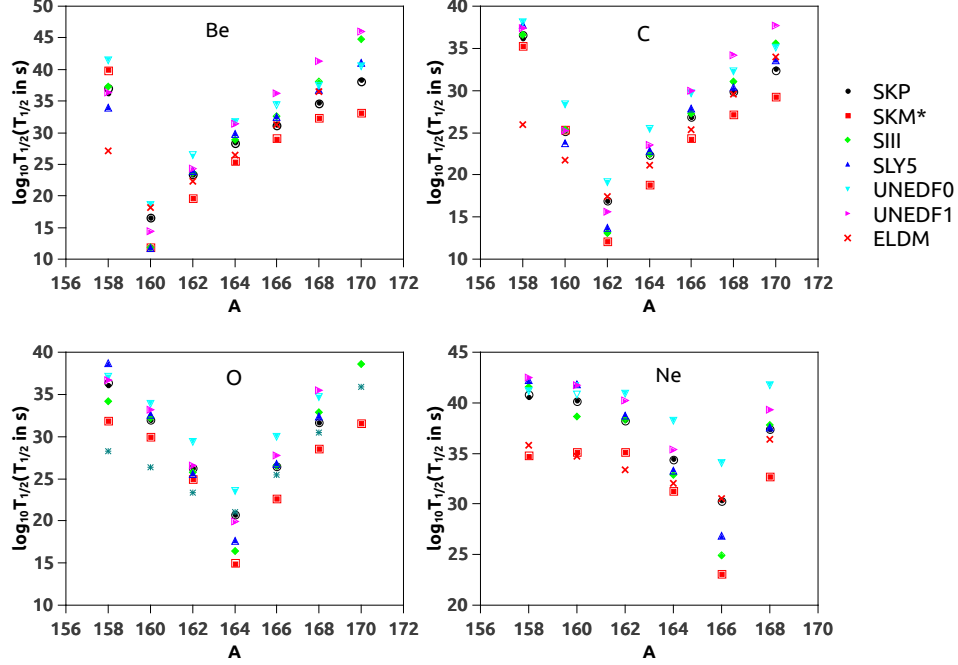


Figure 2: Plots showing logarithmic value of half-life ($T_{1/2}$ in sec) against mass number of parent (A) nuclei, corresponding to different cluster decay modes for HO(solid) and THO(open) basis.

^{16}O :

$$Q(N, Z) = B(N - 8, Z - 8) + B(8, 8) - B(N, Z) \quad (14)$$

^{20}Ne :

$$Q(N, Z) = B(N - 10, Z - 10) + B(10, 10) - B(N, Z) \quad (15)$$

where, $B(N-4, Z-4)$, $B(N-6, Z-6)$, $B(N-8, Z-8)$, $B(N-10, Z-10)$ are the binding energies of the corresponding daughter nuclei (^{70}Yb , ^{68}Er , ^{66}Dy and ^{64}Gd) and $B(4,4)$, $B(6,6)$, $B(8,8)$ and $B(10,10)$ are the binding energies of the clusters ^8Be , ^{12}C , ^{16}O and ^{20}Ne respectively. Q-values calculated with respect to different Skyrme forces are given in Table 3. We have compared the obtained results with the ELDM values. In this case also we have calculated half-lives using UDL and they are depicted in Fig. 2.

The decay rate for a particular decay mode will be maximum, if the corresponding half-life is minimum. From Fig. 2, it is found that in the case of ^8Be decay, the half-life is minimum for ^{160}W . This shows that the decay rate of ^8Be is maximum for ^{160}W isotope. Also, this particular decay leads to the formation of the daughter nucleus, ^{152}Yb which is having magic neutron number ($N=82$). Similarly for ^{12}C , ^{16}O , ^{20}Ne decay modes, half lives are minimum for those decays which leads to the formation of daughter nuclei (i.e, ^{150}Er , ^{148}Dy and ^{146}Gd) having magic neutron number ($N=82$). These results show that the rate of decay will be maximum for those decay modes leading to magic daughter nuclei ($N=82$). These observations confirm the role of magicity in cluster decay.

We have shown the values of half-lives predicted using different Skyrme forces in Fig. 2. All the calculations show similar trend in predicting the values, but with minor discrepancy in their magnitudes. We have estimated the half-lives of all the decay modes from the binding energies of W isotopes, which are obtained using different Skyrme forces. Each Skyrme force predicts the binding energy with a slight variation in its values and it is reflected in the predicted half-lives. All the half-lives except those obtained by SKM* overestimate the ELDM values. From Fig. 2, it is observed that Ne radioactivity half-lives do not fall within the experimentally measurable range. But we have predicted ^{20}Ne as well as ^{24}Mg decay in Os isotopes in our previous work[10] and also in Pt isotopes. This shows that as the parent nuclei becomes massive, we can expect more heavier cluster emissions.

Geiger-Nuttel (GN) plot shows the relation between logarithmic half-lives and the disintegration energy(Q) of different decay modes. Geiger-Nuttel law, which is a linear relation between these two quantities, is given by,

$$\log_{10}T_{1/2} = \frac{X}{\sqrt{Q}} + Y \quad (16)$$

where X and Y are the slopes and intercepts of the straight lines respectively. Fig. 3 shows the GN plots for different clusters emitted from W isotopes corresponding to various Skyrme parameters. The linear nature of the plot is reproduced in the case of all the cluster modes. Each emitted cluster has a

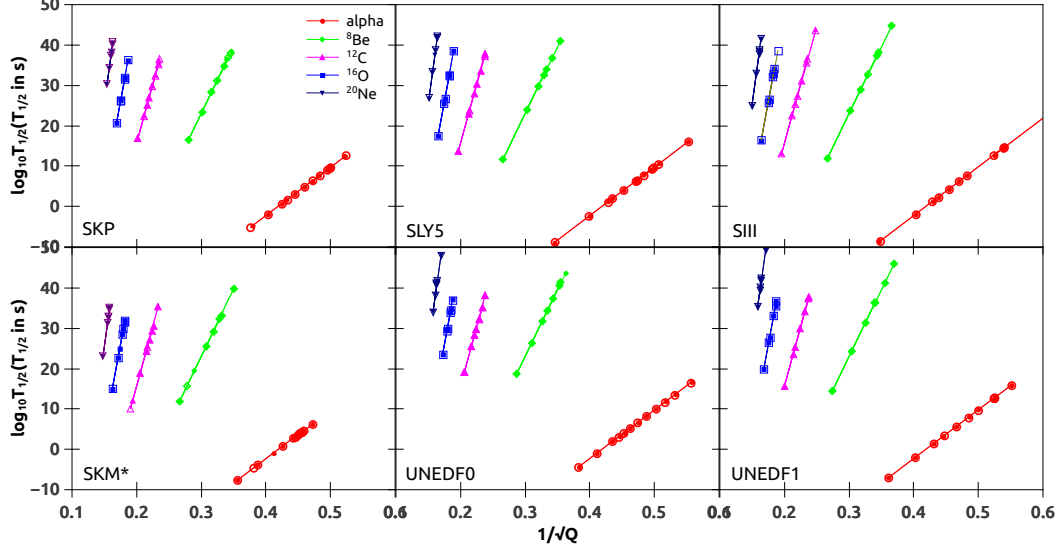


Figure 3: Geiger-Nuttall plots of different cluster decay modes for HO(solid) and THO(open) basis corresponding to different Skyrme forces.

specific slope and intercept. They are given in Table 4. From this table, we can see that as the emitted cluster becomes massive, the slope as well as the intercept increases.

5. Conclusion

In the present work, we have made an attempt to study the sensitivity of different Skyrme parametrizations in predicting the feasibility of alpha decay and cluster decay from W isotopes. A comparative study of half-lives was also done by using two different basis, HO and THO, which are used for solving HFB equations. Both HO and THO basis do not produce much significant difference in the obtained results. We have also compared the results with ELDM, which is a phenomenological model, wherever the experimental values are not available.

We have observed that the trend of the half-lives predicted by different Skyrme forces are similar. Depending on the various factors used for designing

different Skyrme forces, the values of half-lives for different decay modes vary slightly. We can get a qualitative description of alpha and cluster radioactivity using Skyrme HFB approach. The most probable decay in various decay modes leads to magic daughter nuclei with $N=82$. This again confirms the role of magicity in cluster radioactivity. In the present study, we have selected only a few Skyrme forces. The study can be extended to other Skyrme forces also. It is hoped that these results can be a helping guide for the experimentalists in their future research.

Acknowledgments

One of the authors, (NA) gratefully acknowledges UGC, Govt. of India, for providing the grant under UGC-JRF/SRF scheme and also for providing facilities made available under UGC-SAP-DRS II project.

References

- [1] A. Sandulescu, D. N. Poenaru and W. Greiner, *Sov. J. Part. Nucl. II*, **11**, 528 (1980).
- [2] H. J. Rose, G. A. Jones, *Nature (London)* **307** 245(1984).
- [3] R. K. Gupta, *Pramana-J. Phys.* **53** 3(1999).
- [4] W. Greiner, H. J. Fink, J. A. Maruhn and W. Scheid, *Zeitschrift fuer Physik*, **268**, 321(1974).
- [5] S. S. Malik and R. K. Gupta, *Phys. Rev. C*, **39**, 1992(1989).
- [6] D. N. Poenaru, M. Ivascu, A. Sandulescu and W. Greiner, *Phys. Rev. C*, **32**, 572(1985).
- [7] D. A. Eastham and I. S. Grant, *Nucl. Phys. A.*, **208**, 119(1973).
- [8] F. A. Danevich, A. Sh. Georgadze, V. V. Kobychiev, S. S. Nagorny, A. S. Nikolaiko, O. A. Ponkratenko, V. I. Tretyak, S. Yu. Zdesenko, and Yu. G. Zdesenko, *Phys. Rev. C*, **67**, 014310(2003).

- [9] S. Hofmann, W. Faust, G. Munzenberg, W. Reisdorf, P. Armbruster, K. Guttner and H. Ewald, *Zeitschrift fuer Physik*, **291**, 53(1979).
- [10] N. Ashok, D. M. Joseph and A. Joseph, *Mod. Phys. Lett. A*, **31**, 1650045(2016).
- [11] P. Ring and P. Shuck, *The Nuclear Many-Body Problem*, (Springer, Berlin, 1980).
- [12] M. Bender, P.H. Heenen and P.G. Reinhard, *Rev. Mod. Phys*, **75**, 121(2003).
- [13] M.V. Stoitsov, N. Schunck, M. Kortelainen, N. Michel, H. Nam, E. Olsen, J. Sarich, S. Wild, *Comp. Phys. Commun.*, **184**, 1592(2013).
- [14] I. Zh. Petkov and M.V. Stoitsov, *Compt. Rend. Bulg.Acad. Sci.*, **34**, 1651(1981); *Theor. Math. Phys.*, **55**, 584(1983); *Sov. J. Nucl. Phys.*, 37, 692(1983).
- [15] M. V. Stoitsov, J. Dobaczewski, W. Nazarewicz and P. Ring, *Comp. Phys. Commun.*, **167**, 43(2005).
- [16] T. H. R. Skyrme, *Nucl. Phys.*, **9**, 615(1959).
- [17] M. Beiner, H. Flocard, N. Van Giai, and P. Quentin, *Nucl. Phys. A.*, **238**, 29(1975).
- [18] J. Dobaczewski, H. Flocard and J. Treiner, *Nucl. Phys. A*, **422**, 103(1984).
- [19] E. Chabanat, P. Bonche, P. Haensel, J. Meyer and R. Schaeffer, *Nucl. Phys. A*, **627**, 710(1997).
- [20] J. Bartel, P. Quentin, M. Brack, C. Guet, and H. B. Hakansson, *Nucl. Phys. A*, **386**, 79 (1982).
- [21] M. Kortelainen, T. Lesinski, J. More, W. Nazarewicz, J. Sarich, N. Schunck, M.V. Stoitsov and S. Wild, *Phys. Rev. C*, **82**, 024313(2010).

- [22] M. Kortelainen, J. McDonnell, W. Nazarewicz, P.G. Reinhard, J. Sarich, N. Schunck, M.V. Stoitsov and S. Wild, *Phys. Rev. C*, **85**, 024304(2012).
- [23] R.R. Chasman, *Phys. Rev. C*, **14**, 1935(1976).
- [24] J.Terasaki, P.H. Heenen, P. Bonche, J. Dobaczewski and H. Flocard, *Nucl. Phys. A*, **593**, 1(1995).
- [25] J. Dobaczewski, W. Nazarewicz and M.V. Stoitsov, *Eur. Phys. J. A*, **15**, 21(2002).
- [26] J.Terasaki, H. Flocard, P.H. Heenen and P. Bonche, *Nucl. Phys. A*, **621**, 706(1997).
- [27] Dongdong Ni, Zhongzhou Ren, Tiekuan Dong and Chang Xu, *Phys.Rev. C*, **78**, 044310(2008).
- [28] M. Wang, G. Audi, A. H. Wapstra, F. G. Kondev, M. MacCormick, X. Xu, and B. Pfeiffer, *CPC*, **36**, 12(2012).
- [29] M. Goncalves and S. B. Duarte, *Phys. Rev. C* **48**, 2409(1993).
- [30] M. Goncalves, S. B. Duarte, F. Garcia, O. Rodriguez, *Comp. Phys. Commun.*, **107**, 246(1997).
- [31] D. A. Eastham and I. S. Grant, *Nucl. Phys. A*, **208**, 119(1973).
- [32] F.A. Danevich, A.Sh. Georgadze, V.V. Kobychiev, S.S. Nagorny, A.S. Nikolaiko, O.A. Ponkratenko, V.I. Tretyak, S.Yu. Zdesenko, Yu.G. Zdesenko, P.G. Bizzeti, T.F. Fazzini and P.R. Maurenzig, *Phys. Rev. C*, **67**, 014310(2003).

Table 1: Q-values of alpha decay in even-even W isotopes calculated with Skyrme HFB equations solved using HO(top) and THO(bottom) basis along with ELDM and available experimental values.

| Alpha decay | Q value | | | | | | | |
|---|---------|--------|--------|--------|--------|--------|--------|---------------------------|
| | SIII | SKP | SkM* | SLy5 | UNEDF0 | UNEDF1 | ELDM | exp |
| $^{158}\text{W} \rightarrow \alpha + ^{154}\text{Hf}$ | 8.2843 | 7.0719 | 7.9058 | 8.3707 | 6.8296 | 7.6901 | 6.6051 | |
| | 8.2448 | 6.9272 | 7.9024 | 8.3608 | 6.8330 | 7.6648 | | |
| $^{160}\text{W} \rightarrow \alpha + ^{156}\text{Hf}$ | 6.1670 | 6.1679 | 6.6801 | 6.2786 | 5.9269 | 6.1993 | 6.0651 | |
| | 6.1674 | 6.1565 | 6.6793 | 6.2924 | 5.9236 | 6.1915 | | |
| $^{162}\text{W} \rightarrow \alpha + ^{158}\text{Hf}$ | 5.4312 | 5.5584 | 5.8998 | 5.4535 | 5.2839 | 5.3959 | 5.6781 | 5.53 ^(ref.31) |
| | 5.4375 | 5.5595 | 5.9009 | 5.4641 | 5.2811 | 5.3908 | | |
| $^{164}\text{W} \rightarrow \alpha + ^{160}\text{Hf}$ | 5.2161 | 5.3343 | 5.5125 | 5.2823 | 5.0426 | 5.0211 | 5.2781 | 5.153 ^(ref.31) |
| | 5.2140 | 5.3451 | 5.5043 | 5.2808 | 5.0586 | 5.0135 | | |
| $^{166}\text{W} \rightarrow \alpha + ^{162}\text{Hf}$ | 4.8437 | 5.0529 | 5.1203 | 4.8793 | 4.8716 | 4.6123 | 4.8561 | |
| | 4.8417 | 5.0623 | 5.1196 | 4.8811 | 4.8872 | 4.6160 | | |
| $^{168}\text{W} \rightarrow \alpha + ^{164}\text{Hf}$ | 4.5294 | 4.7429 | 4.8816 | 4.5113 | 4.6839 | 4.2422 | 4.5001 | |
| | 4.5225 | 4.7255 | 4.8851 | 4.5205 | 4.6878 | 4.2600 | | |
| $^{170}\text{W} \rightarrow \alpha + ^{166}\text{Hf}$ | 4.3104 | 4.4892 | 4.8444 | 4.2749 | 4.4489 | 3.9996 | 4.1441 | |
| | 4.3094 | 4.4941 | 4.8412 | 4.2828 | 4.4591 | 4.0115 | | |
| $^{172}\text{W} \rightarrow \alpha + ^{168}\text{Hf}$ | 3.4093 | 4.2776 | 4.7594 | 4.0082 | 4.2088 | - | 3.8391 | |
| | 3.4486 | 4.2899 | 4.7566 | 4.0265 | 4.2107 | - | | |
| $^{174}\text{W} \rightarrow \alpha + ^{170}\text{Hf}$ | 3.6332 | 4.0139 | 5.0409 | 3.8931 | 3.9625 | 3.6108 | 3.6021 | |
| | 3.6458 | 4.0131 | 5.0231 | 3.9034 | 3.9671 | 3.6265 | | |
| $^{176}\text{W} \rightarrow \alpha + ^{172}\text{Hf}$ | 3.4270 | 4.0882 | 4.9569 | 4.4733 | 3.7381 | 3.6371 | 3.3351 | |
| | 3.4492 | 4.0904 | 4.9373 | 4.4529 | 3.7501 | 3.6459 | | |
| $^{178}\text{W} \rightarrow \alpha + ^{174}\text{Hf}$ | 3.4460 | 4.0156 | 4.8358 | 4.0885 | 3.5356 | 3.6378 | 3.0128 | |
| | 3.4257 | 4.0211 | 4.8235 | 4.0597 | 3.5539 | 3.6392 | | |
| $^{180}\text{W} \rightarrow \alpha + ^{176}\text{Hf}$ | 2.4381 | 3.6434 | 4.4935 | 3.2756 | 3.2196 | 3.2942 | 2.5149 | 2.516 ^(ref.32) |
| | 2.4365 | 3.6597 | 4.4771 | 3.2793 | 3.2383 | 3.2923 | | |

Table 2: Comparison of standard deviation of alpha decay half-lives of W isotopes calculated for different Skyrme forces

| | SKP | SLY5 | SIII | SKM* | UNEDF0 | UNEDF1 |
|-----|--------|--------|--------|--------|--------|--------|
| HO | 1.0088 | 0.8719 | 0.6646 | 2.0293 | 0.9245 | 0.9828 |
| THO | 1.0278 | 0.8850 | 0.6540 | 2.0208 | 0.9281 | 0.9850 |

Table 3: Same as Table 1, but for various clusters

| Cluster decay | Q value | | | | | | |
|---|--------------------|--------------------|--------------------|--------------------|--------------------|--------------------|---------|
| | SIH | SKP | SKM* | SLy5 | UNEDF0 | UNEDF1 | ELDM |
| $^{158}\text{W} \rightarrow ^8\text{Be} + ^{150}\text{Yb}$ | 8.5165 8.5196 | 8.6746 8.5584 | 8.1450 8.1576 | 9.0354 9.0398 | 7.9249 7.9364 | 7.5949 8.6686 | 9.9983 |
| $^{160}\text{W} \rightarrow ^8\text{Be} + ^{152}\text{Yb}$ | 14.1145 14.0845 | 12.7116 12.7087 | 14.1092 14.0999 | 14.1472 14.1462 | 12.1651 12.1749 | 13.3722 13.3233 | 11.9983 |
| $^{162}\text{W} \rightarrow ^8\text{Be} + ^{154}\text{Yb}$ | 10.9519 10.9602 | 11.0198 11.0270 | 11.9117 11.9146 | 10.8985 10.9209 | 10.3995 10.3887 | 10.8471 10.8340 | 10.9903 |
| $^{164}\text{W} \rightarrow ^8\text{Be} + ^{156}\text{Yb}$ | 9.8920 9.9013 | 9.9878 10.0048 | 10.5721 10.5653 | 9.7219 9.7282 | 9.3746 9.3851 | 9.4569 9.4439 | 10.0883 |
| $^{166}\text{W} \rightarrow ^8\text{Be} + ^{158}\text{Yb}$ | 9.2564 9.2178 | 9.4512 9.4752 | 9.8530 9.8442 | 9.2583 9.2523 | 8.9077 8.9298 | 8.6402 8.6371 | 9.1803 |
| $^{168}\text{W} \rightarrow ^8\text{Be} + ^{160}\text{Yb}$ | 8.3727 8.3601 | 8.8660 8.8807 | 9.2632 9.2667 | 8.5529 8.5514 | 8.4527 8.4652 | 7.9136 7.9185 | 8.3303 |
| $^{170}\text{W} \rightarrow ^8\text{Be} + ^{162}\text{Yb}$ | 7.4664 7.4601 | 8.3119 8.3565 | 9.1163 9.1158 | 7.9436 7.9457 | 7.9983 8.0080 | 7.3057 7.3135 | 7.5953 |
| $^{158}\text{W} \rightarrow ^{12}\text{C} + ^{146}\text{Er}$ | 18.0288 18.0469 | 18.1709 18.0619 | 18.3956 18.4012 | 17.7180 17.7474 | 17.6459 17.6648 | 17.8516 17.8583 | 20.622 |
| $^{160}\text{W} \rightarrow ^{12}\text{C} + ^{148}\text{Er}$ | 21.3810 21.3880 | 21.4193 21.4263 | 21.3479 21.3589 | 21.8918 21.9185 | 20.3908 20.3914 | 21.4069 21.3912 | 22.099 |
| $^{162}\text{W} \rightarrow ^{12}\text{C} + ^{150}\text{Er}$ | 26.1713 26.1485 | 24.4897 24.4849 | 26.5842 26.5816 | 25.8829 25.8869 | 23.5826 23.5932 | 25.0532 25.0148 | 23.831 |
| $^{164}\text{W} \rightarrow ^{12}\text{C} + ^{152}\text{Er}$ | 22.3285 22.3298 | 22.3276 22.3407 | 23.6660 23.6585 | 22.1521 22.1721 | 21.2683 21.2761 | 21.9540 21.9438 | 22.266 |
| $^{166}\text{W} \rightarrow ^{12}\text{C} + ^{154}\text{Er}$ | 20.6668 20.6676 | 20.7735 20.7931 | 21.6400 21.6318 | 20.4620 20.4656 | 19.8958 19.9143 | 19.8242 19.8154 | 20.717 |
| $^{168}\text{W} \rightarrow ^{12}\text{C} + ^{156}\text{Er}$ | 19.4806 19.4665 | 19.8267 19.8336 | 20.6571 20.6541 | 19.6931 19.6781 | 19.1118 19.1288 | 18.5680 18.5744 | 19.317 |
| $^{170}\text{W} \rightarrow ^{12}\text{C} + ^{158}\text{Er}$ | 18.1849 18.1726 | 19.0182 19.0666 | 19.9845 19.9816 | 18.7305 18.7168 | 18.2899 18.3092 | 17.6292 17.649 | 18.014 |
| $^{158}\text{W} \rightarrow ^{16}\text{O} + ^{142}\text{Dy}$ | 29.5101 29.5086 | 28.8028 28.6975 | 30.3917 30.3727 | 27.9216 27.9127 | 28.4526 28.4691 | 28.4691 28.5935 | 31.157 |
| $^{160}\text{W} \rightarrow ^{16}\text{O} + ^{144}\text{Dy}$ | 30.1986 30.2093 | 30.3007 30.3126 | 31.0786 31.0895 | 30.0405 30.0739 | 29.5483 29.5663 | 29.5663 29.8251 | 31.927 |
| $^{162}\text{W} \rightarrow ^{16}\text{O} + ^{146}\text{Dy}$ | 32.7798 32.7960 | 32.5919 32.5986 | 33.1311 33.1432 | 32.8781 32.8958 | 31.2475 31.2867 | 31.2867 32.4321 | 33.292 |
| $^{164}\text{W} \rightarrow ^{16}\text{O} + ^{148}\text{Dy}$ | 37.2166 37.2017 | 35.0472 35.0540 | 37.9786 37.9577 | 36.5910 36.5940 | 33.7072 33.7293 | 33.7293 35.4355 | 34.362 |
| $^{166}\text{W} \rightarrow ^{16}\text{O} + ^{150}\text{Dy}$ | 32.3325 32.3346 | 32.3992 32.4169 | 34.0840 34.0689 | 32.2562 32.2685 | 30.9283 30.9418 | 30.9418 31.8396 | 32.158 |
| $^{168}\text{W} \rightarrow ^{16}\text{O} + ^{152}\text{Dy}$ | 29.7736 29.7726 | 30.2490 30.2534 | 31.4556 31.4505 | 29.9717 29.9762 | 29.1075 29.1339 | 29.1339 28.8249 | 29.962 |
| $^{170}\text{W} \rightarrow ^{16}\text{O} + ^{154}\text{Dy}$ | 27.7213 27.7212 | 28.7941 28.8416 | 30.2402 30.2304 | 28.8077 28.7877 | 27.9051 27.9333 | 27.1763 - | 27.841 |
| $^{158}\text{W} \rightarrow ^{20}\text{Ne} + ^{138}\text{Gd}$ | 37.4084 37.4142 | 37.8199 37.7133 | 40.2825 40.2517 | 37.1795 37.1381 | 37.5530 37.5530 | 37.0624 37.0619 | 35.7945 |
| $^{160}\text{W} \rightarrow ^{20}\text{Ne} + ^{140}\text{Gd}$ | 38.5361 38.5313 | 37.8979 37.9152 | 40.0555 40.0393 | 37.2569 37.2690 | 37.2671 37.2671 | 37.2925 37.2945 | 34.6913 |
| $^{162}\text{W} \rightarrow ^{20}\text{Ne} + ^{142}\text{Gd}$ | 38.6017 38.6242 | 38.6360 38.6508 | 39.9717 39.9862 | 38.4065 38.4521 | 37.5541 37.5541 | 37.8696 37.8534 | 33.3599 |
| $^{164}\text{W} \rightarrow ^{20}\text{Ne} + ^{144}\text{Gd}$ | 40.9146 40.9272 | 40.2224 40.2396 | 41.6357 41.6361 | 40.6858 40.7305 | 38.5794 38.5794 | 39.8443 39.8258 | 32.0253 |
| $^{166}\text{W} \rightarrow ^{20}\text{Ne} + ^{146}\text{Gd}$ | 44.7203 44.7027 | 42.0287 42.0382 | 45.6637 45.6402 | 43.7478 43.7349 | 40.3151 40.3151 | - - | 30.5302 |
| $^{168}\text{W} \rightarrow ^{20}\text{Ne} + ^{148}\text{Gd}$ | 38.6716 38.6858 | 38.8529 38.8553 | 40.8899 40.8805 | 38.7856 38.7894 | 37.0623 37.0623 | 38.0478 38.0478 | 36.3782 |

Table 4: Slopes and intercepts of even-even W isotopes calculated for different Skyrme forces

| Skyrme force | Alpha | | Be | | C | | O | | Ne | |
|-----------------|---------|-----------|---------|-----------|---------|-----------|---------|-----------|----------|-----------|
| | Slope | Intercept | Slope | Intercept | Slope | Intercept | Slope | Intercept | Slope | Intercept |
| SKP | 119.866 | -50.212 | 330.189 | -76.060 | 580.124 | -100.322 | 879.117 | -127.861 | 1206.770 | -155.868 |
| | 119.803 | -50.182 | 330.406 | -76.060 | 580.572 | -100.422 | 879.117 | -127.861 | 1206.770 | -155.870 |
| SLY5 | 120.559 | -50.524 | 330.200 | -76.062 | 581.055 | -100.525 | 875.289 | -127.181 | 1190.031 | -153.194 |
| | 120.546 | -50.187 | 330.198 | -76.061 | 580.972 | -100.507 | 875.271 | -127.177 | 1193.551 | -153.683 |
| SIII | 121.191 | -50.779 | 330.727 | -76.223 | 580.500 | -100.390 | 872.011 | -126.587 | 1184.827 | -152.336 |
| | 121.182 | -50.776 | 330.715 | -76.219 | 580.449 | -100.378 | 860.188 | -124.536 | 1185.006 | -152.364 |
| SKM* | 119.353 | -50.063 | 331.083 | -76.390 | 583.610 | -101.112 | 866.964 | -125.747 | 1193.181 | -153.544 |
| | 119.605 | -50.179 | 331.793 | -76.589 | 583.614 | -101.114 | 865.863 | -125.553 | 1195.265 | -153.856 |
| UNEDF0 | 120.241 | -50.352 | 329.901 | -75.953 | 584.205 | -101.176 | 876.459 | -127.421 | 1135.247 | -144.43 |
| | 120.218 | -50.343 | 330.861 | -76.254 | 584.219 | -101.179 | 876.473 | -127.422 | 1132.531 | -143.99 |
| UNEDF1 | 120.561 | -50.492 | 330.377 | -76.093 | 582.262 | -100.744 | 871.549 | -126.519 | 1131.420 | -143.772 |
| | 120.545 | -50.485 | 330.357 | -76.087 | 582.248 | -100.741 | 871.161 | -126.531 | 1131.304 | -143.753 |